Crustal structure and implications for the tectonic evolution of the Archean Western Superior craton from forward and inverse gravity modeling

B. Nitescu,[1] A. R. Cruden,[1] and R. C. Bailey[1,2]

Received 22 July 2004; revised 31 October 2005; accepted 29 November 2005; published 23 February 2006.

[1] The distribution of mass anomalies within the crust of the Archean Western Superior Province has been investigated with forward and inverse gravity modeling routines. The gravity models indicate that in most of the Western Superior Province, significant mass anomalies occur only within the top 10 km of the crust, where they are generally related to dense metavolcanic rocks and low-density granitoid plutons, and at the crust-mantle boundary, where they are linked to undulations of this interface. An exception is the region encompassing the central Wabigoon Subprovince and the segments of the Quetico and Wawa belts south of it, where implied large intracrustal mass anomalies are associated with a segment of denser lower crust, and with overlying depressions of the interfaces between the main crustal layers. We interpret the predominant lateral mass homogeneity observed at deep crustal levels as evidence of mass redistribution processes associated with a major postaccretionary episode of thermal softening of the Western Superior crust. The incongruent presence of a denser lower crustal segment may reflect the subsequent modification of the lower crust through magmatic intra and underplating, possibly in relation with the Mesoproterozoic midcontinent rifting event. **Citation:** Nitescu, B., A. R. Cruden, and R. C. Bailey (2006), Crustal structure and implications for the tectonic evolution of the Archean Western Superior craton from forward and inverse gravity modeling, *Tectonics*, *25*, TC1009, doi:10.1029/2004TC001717.

1. Introduction

[2] The remarkable lithological, metamorphic and structural characteristics of the Archean cratons (e.g., the exceptionally large volume of granitoids; the lack of convincing examples of modern-style passive margin sequences, ophiolites, accretionary prisms and mélange belts; the absence of high-pressure, low-temperature metamorphism; the dome-and-basin geometry of the granite-greenstone terrains) have long been considered indicators of processes of crustal formation and evolution fundamentally different from those of the Phanerozoic time. While this might have been the case for the Mesoarchean and older continental masses [e.g., *Zegers and van Keken*, 2001], it appears on the basis of seismic data acquired during the past two decades in the Abitibi-Opatica belts of the Superior craton and in the southwestern Yilgarn craton [e.g., *Calvert et al.*, 1995; *Wilde et al.*, 1996; *Dentith et al.*, 2000] that the growth of Neoarchean continents occurred through lateral accretionary processes having similarities to those observed in the modern rock record.

[3] More recent suggestions in this sense came from the western part of the Superior Province (Figure 1), where Lithoprobe seismic observations [*White et al.*, 2003; *Calvert et al.*, 2004] are consistent with a proposed interpretation of the Western Superior Province (WS) on the basis of geochronological, geochemical, and field investigations [e.g., *Langford and Morin*, 1976; *Card*, 1990; *Williams*, 1990; *Williams et al.*, 1992; *Card and Poulsen*, 1998] as the result of a process of progressive growth by lateral accretion of various arc and continental fragments. However, despite the important insight provided by Lithoprobe seismic data, an understanding of the crustal structure and tectonic evolution of the Western Superior Province based solely on this type of deep information is difficult. Although the relative ages of reflections and sometimes their nature can be inferred from apparent truncations [e.g., *Calvert et al.*, 2004], their true age and significance are in most cases equivocal, especially at deep levels, where reflections cannot be tied to surface structures. As is the case in the majority of younger orogens, it is likely that the complex pattern of reflectivity observed in the WS crust is partly related to the overprinting of accretionary structures by processes that occurred at different stages of its postaccretionary evolution.

[4] A source of information on the deep structure and evolution of the crust that is complementary to seismic data is the gravity field. While lacking the structural detail provided by seismic data, and in spite of the ambiguity in its interpretation, the gravity field can be used to constrain the distribution of mass within the crust, and implicitly to bring a new perspective on the processes that affected the crust, if constraints from surface observations (e.g., rock densities, surface extent of geological bodies) and seismic data (e.g., rock velocities, geometry of structures) are available. In the current study, given the availability of constraints from deep Lithoprobe seismic reflection and

[1]Department of Geology, University of Toronto, Toronto, Ontario, Canada.
[2]Department of Physics, University of Toronto, Toronto, Ontario, Canada.

0278-7407/06/2004TC001717

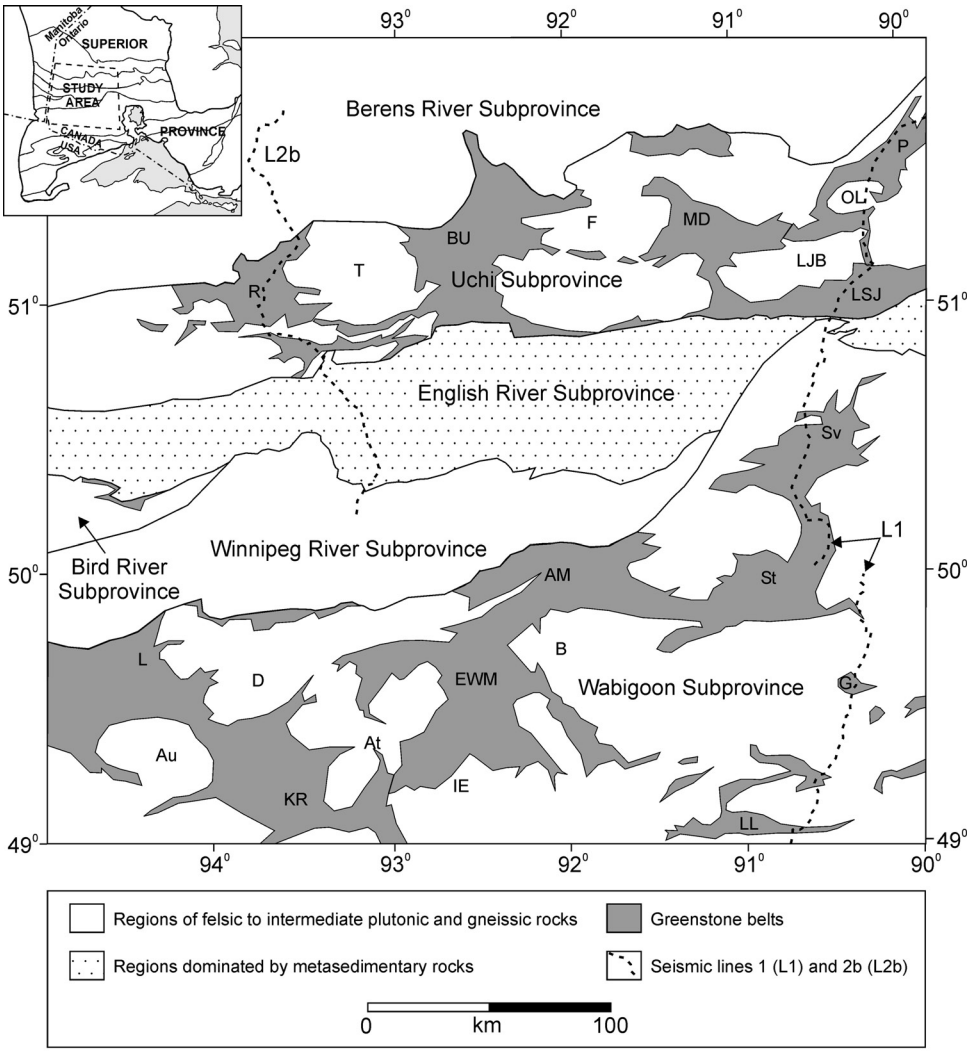

Figure 1. Schematic map of the Western Superior Province in the area of study. AM, Abram-Minnitaki greenstone belt; At, Atikwa batholith; Au, Aulneau batholith; B, Basket Lake batholith; BU, Birch-Uchi greenstone belt; D, Dryberry batholith; EWM, Eagle-Wabigoon-Manitou greenstone belt; F, Fawcett Lake batholith; G, Garden Lake greenstone belt; IE, Irene-Eltrut batholith; KR, Kakagi-Rowan greenstone belt; L, Lake of the Woods greenstone belt; LJB, Lake St. Joseph batholith; LL, Lumby Lake greenstone belt; LSJ, Lake St. Joseph greenstone belt; MD, Meen-Dempster greenstone belt; OL, Ochig Lake pluton; P, Pickle Lake greenstone belt; R, Red Lake greenstone belt; St, Sturgeon Lake greenstone belt; Sv, Savant Lake greenstone belt; T, Trout Lake batholith.

seismic refraction data (e.g., Moho topography, crustal velocity model), we investigate the structure of the WS crust by using forward modeling of gravity data collected along two extensive, north-south trending Lithoprobe seismic profiles (lines 1 and 2b, Figure 1), as well as inverse modeling of the regional gravity data set. The gravity modeling is intended to provide information on the occurrence of gross lateral density variations within the deeper crustal levels of crust, the relationships at depth between the WS belts, and the characteristic depth ranges of the exposed upper crustal bodies. Clarification of such aspects of the crustal structure can ultimately have important implications for the understanding of the role of accretionary and postaccretionary tectonic processes in the evolution of the WS crust. The specific area of investigation on which this study is focused extends between 49°N and 52°N and between 90°W and 95°W, and covers the western halves of the Berens River, Uchi, English River, Winnipeg River, and Wabigoon subprovinces (Figure 1).

2. Geologic Background

2.1. Regional Characteristics

[5] The western part of the Superior Province (Figure 1) comprises a regional succession of alternating, east-west

striking granite-greenstone (volcano-plutonic), metasedimentary and metaplutonic belts (subprovinces) that have distinct lithological, structural, metamorphic and geophysical attributes [*Card and Ciesielski*, 1986]. The granite-greenstone subprovinces (e.g., Uchi, Bird River, Wabigoon subprovinces) are characterized by supracrustal sequences of metavolcanic and subordinate metasedimentary rocks known as greenstone belts that are surrounded and cut by granitoid plutons (Figure 1). Most of the metavolcanic rocks in the WS were erupted between 2.75 and 2.71 Ga [e.g., *Davis*, 1998], but older (2.8–3.0 Ga) metavolcanics also occur. The plutonic rocks that surround and intrude the greenstone belts include mostly synvolcanic to postorogenic granitoids. The metamorphic grade of these regions is generally in the greenschist to subgreenschist facies. The metasedimentary subprovinces (English River Subprovince and Quetico Subprovince) consist of variably deformed and metamorphosed pre-2.69 Ga accumulations of immature clastic sediments derived from adjacent volcano-plutonic domains. These terrains are characterized, for the most part, by relatively low pressure amphibolite- to granulite-grade metamorphic conditions and widespread partial melting of the metasedimentary gneiss. The metaplutonic subprovinces (Berens River and Winnipeg River subprovinces) are regions dominated by intermediate to felsic plutonic rocks that were affected by medium- to high-grade regional metamorphism. In the Berens River Subprovince, most of the plutonic rocks have ages of 2.75–2.69 Ga and were emplaced into an older (2.8–3.0 Ga) crustal domain of plutonic and volcanic rocks, from which only small remnants are preserved [*Corfu and Stone*, 1998]. In the Winnipeg River Subprovince, which is a cratonic segment that contains the oldest crustal components documented so far in the WS, magmatic activity began as early as 3.3 Ga and continued intermittently to circa 2.66 Ga [*Krogh et al.*, 1976; *Corfu*, 1988; *Beakhouse*, 1991; *Cruden et al.*, 1998; *Melnyk et al.*, 2006].

2.2. Tectonic Interpretation

[6] Some early models [e.g., *Langford and Morin*, 1976] and most of the tectonic interpretations in the past two decades [e.g., *Hoffman*, 1989; *Card*, 1990; *Williams*, 1990; *Williams et al.*, 1992; *Card and Poulsen*, 1998] suggest on the basis of observations derived from geochronological, geochemical and field studies (e.g., generally southward younging Neoarchean magmatism, deformation and sedimentation; compositional and geochemical similarities between greenstone belt sequences and modern volcanic arcs) that the growth of the WS occurred mainly through progressive lateral accretion of arc and microcontinental fragments to the southern margin of a Mesoarchean continental block, termed the North Caribou protocraton [*Thurston et al.*, 1991]. The Neoarchean development of the Berens River and Uchi belts on the southern margin of the North Caribou protocraton appears comparable with that of an Andean-type continental margin [*Corfu and Stott*, 1993; *Corfu and Stone*, 1998]. The volcano-plutonic complexes of the Uchi Subprovince record episodic growth between circa 2900 and 2700 Ma, which ended with their deformation between 2720 and 2700 Ma [*Corfu and Stott*, 1993]. The deformation of the Uchi crust was likely caused by far-field stresses transmitted through the Winnipeg River terrain, following the juxtaposition of Neoarchean volcanic assemblages of the western Wabigoon Subprovince with the Winnipeg River belt at circa 2717 Ma [*Melnyk et al.*, 2006]. The English River metasedimentary rocks intervening between the Uchi and Winnipeg River belts appear on the basis of geochronological and field constraints [e.g., *Corfu et al.*, 1995] to represent remnants of sediments deposited in the interval 2715–2698 Ma, as a result of the deformation, uplift and erosion of the Uchi volcano-plutonic complexes. To the south of the Wabigoon Subprovince, the metasediments of the Quetico Subprovince represent a second major accumulation of synorogenic clastic sediments, which records the deformation, uplift and erosion of the Wabigoon volcanic sequences at circa 2700–2690 Ma [*Davis et al.*, 1990], likely following the accretion of the Wawa volcanic arc. The growth of the WS appears to have ended at circa 2680 Ma with a terminal collisional event between the southern margin of the Wawa volcano-plutonic arc with a Paleoarchean to Mesoarchean crustal block (i.e., the circa 3.6–3.0 Ga Minnesota River Valley gneiss terrain).

3. Geophysical Background

3.1. Gravity Data

[7] In the area of study the Bouguer gravity map (Figure 2) shows variations in gravity between −10 and −90 mGal. Comparing the distribution of the gravity anomalies with the mapped geology (Figure 1) indicates that most of the gravity highs occur over greenstone belts, which typically comprise dense metavolcanic rocks (2850–3100 kg/m^3), while the gravity lows correspond to regions underlain by low-density felsic intrusions (2610–2680 kg/m^3). Previous quantitative interpretations of some of these gravity anomalies suggest that the greenstone belts usually extend to depths between 2 and 4 km, whereas the granitoid intrusions that surround them extend to depths ranging between 2 and 15 km [e.g., *Szewczyk*, 1974; *Dusanowskyj*, 1976; *Brisbin and Green*, 1980; *Gupta and Wadge*, 1986].

[8] The most prominent gravity anomaly observed in the WS is a gravity high (>25 mGal) largely coincident with the English River belt (E in Figure 2). Although initially interpreted as the effect of a thick package of metasediments on the basis of a positive surface density contrast (∼40–50 kg/m^3) observed between the English River metasedimentary rocks and the felsic rocks of the neighboring domains [e.g., *Gupta and Barlow*, 1984; *Gupta and Wadge*, 1986], the English River anomaly is likely not an effect of the metasedimentary rocks, since it also extends over felsic intrusions and tonalitic gneisses of the metaplutonic Winnipeg River belt [*Nitescu and Cruden*, 2001; *Nitescu et al.*, 2006]. A recent integrated analysis of magnetic, seismic and gravity information in the English River belt [*Nitescu et al.*, 2006] suggests that this gravity anomaly is caused by a dense charnockitic unit formed within an extensive suite of circa 2698 Ma felsic plutons that intrude the metasedimentary

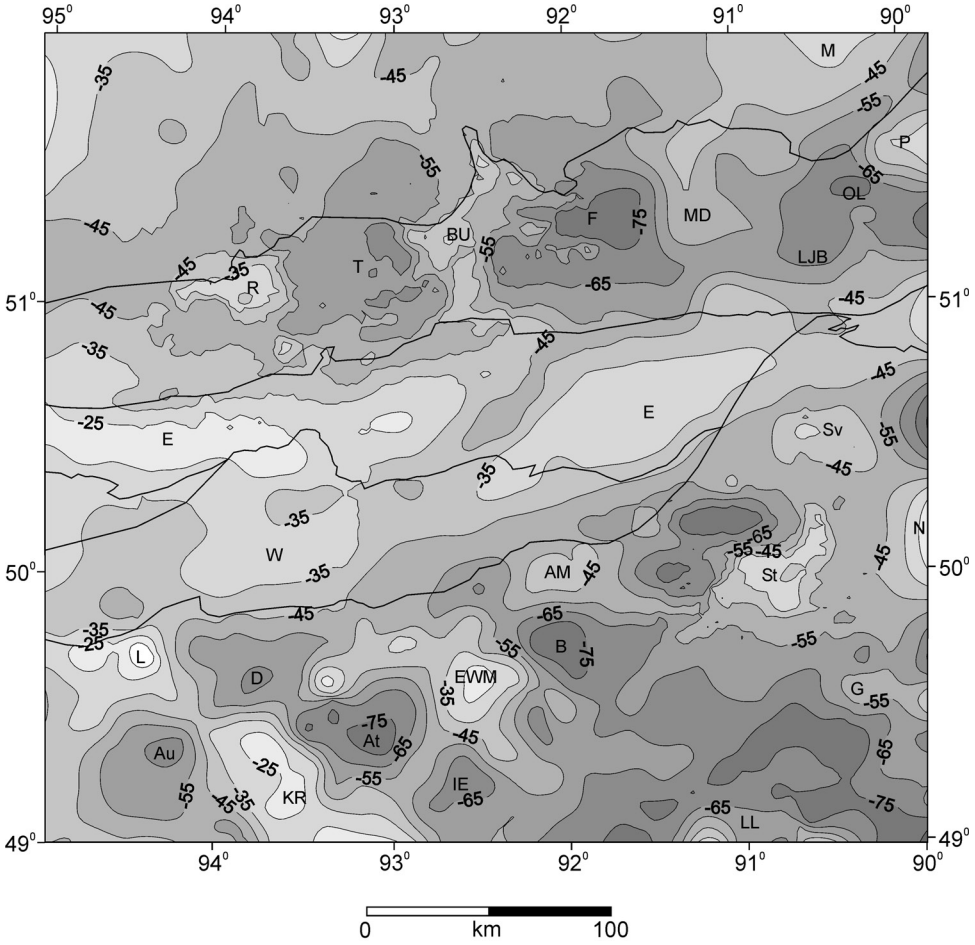

Figure 2. Map of the Bouguer gravity field in the area of study. Contour interval is 10 mGal. The boundaries of the Western Superior belts are also shown. AM, Abram-Minnitaki anomaly; At, Atikwa anomaly; Au, Aulneau anomaly; B, Basket Lake anomaly; BU, Birch-Uchi anomaly; D, Dryberry anomaly; E, English River anomaly; EWM, Eagle-Wabigoon-Manitou anomaly; F, Fawcett Lake anomaly; G, Garden Lake anomaly; IE, Irene-Eltrut anomaly; KR, Kakagi-Rowan anomaly; L, Lake of the Woods anomaly; LJB, Lake St. Joseph anomaly; LL, Lumby Lake anomaly; M, Menako Lake anomaly; MD, Meen-Dempster anomaly; N, anomaly related to Lake Nipigon intrusive rocks; OL, Ochig Lake anomaly; P, Pickle Lake anomaly; R, Red Lake anomaly; St, Sturgeon Lake anomaly; Sv, Savant Lake anomaly; T, Trout Lake anomaly; W, Winnipeg River anomaly.

rocks, in response to high-grade metamorphic conditions attained at circa 2691 Ma. Another significant gravity anomaly produced by a source that is not exposed at surface occurs in the Winnipeg River Subprovince between 93.3°W and 94.3°W (W in Figure 2), in an area that is mostly underlain by a large late orogenic granitic intrusion characterized by lower densities compared to the surrounding rock bodies [e.g., *Gupta and Barlow*, 1984]. It is possible that this anomaly is related to denser upper to middle crustal rocks that were uplifted with respect to the English River belt, as was suggested by early seismic refraction results [*Hall and Hajnal*, 1969, 1973], as well as by a recent interpretation of seismic reflection data collected along Lithoprobe line 2b [*Calvert et al.*, 2004].

[9] The Bouguer gravity field of the WS contains, in addition to numerous gravity effects of upper crustal bodies (e.g., greenstone belts, granitoid plutons), gravity anomalies produced by deeper sources that are generally masked by the effects of shallow origin. *Nitescu et al.* [2003] have shown that these deep effects are largely related to the topography of the crust-mantle boundary. It remains, however, unclear if there are any contributions to the WS gravity field from deep intracrustal sources, and therefore the identification and investigation of such effects constitutes one of the principal objectives of the present study.

3.2. Seismic Data

[10] As part of the Western Superior Lithoprobe transect, both near-vertical-incidence deep (32 s) reflection seismic data and wide-angle reflection–refraction seismic data were

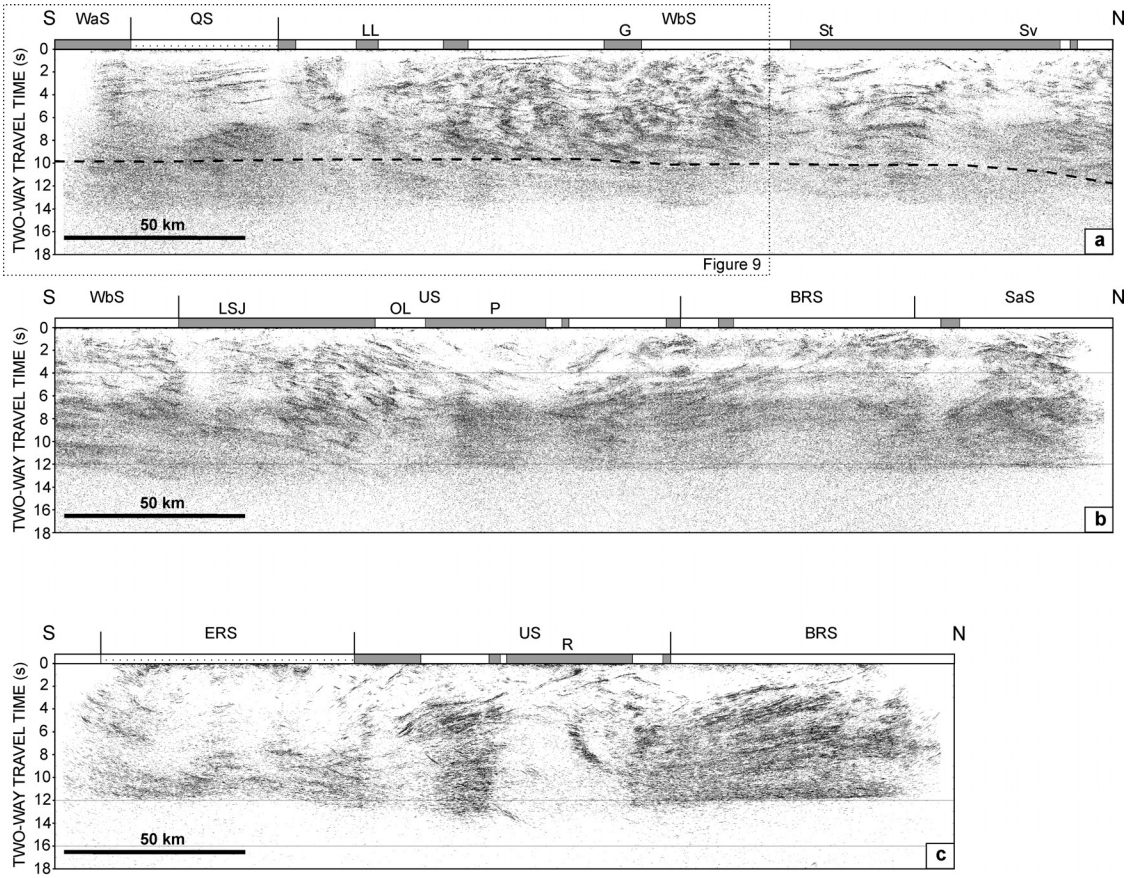

Figure 3. Migrated seismic reflection sections corresponding to (a) the southern and (b) the northern halves of the Lithoprobe seismic line 1, as well as to (c) Lithoprobe seismic line 2b. The dashed line superposed on Figure 3a indicates the top of the anisotropic lower crustal layer revealed by the spatially coincident refraction–wide-angle reflection data. The simplified surface lithology along the profiles is indicated by a horizontal bar with shading and labels similar to those of Figure 1, and the boundaries between subprovinces are indicated by vertical segments. WaS, Wawa Subprovince; QS, Quetico Subprovince; WbS, Wabigoon Subprovince; ERS, English River Subprovince; US, Uchi Subprovince; BRS, Berens River Subprovince; SaS, Sachigo Subprovince. The Lithoprobe seismic data are available online at www.litho.ucalgary.ca/atlas/atlas.html.

acquired along profiles perpendicular and parallel to the strike of the regional succession of metaplutonic, granite-greenstone, and metasedimentary subprovinces.

[11] The near-vertical-incidence seismic reflection data acquired along Lithoprobe lines 1 and 2b [*White et al.*, 2003; *Calvert et al.*, 2004], which are the longest seismic reflection profiles in the WS, indicate a broad threefold layering of the crust, based on the pattern of seismic reflectivity (Figure 3). In the lower part of the crust the reflectivity is generally homogeneous and subhorizontal to shallow dipping and has moderate to high strength. In the middle crust the reflectivity is also moderate to strong, but shows significant lateral heterogeneity imparted by variations in its strength and (or) dip. The upper part of the crust is characterized by numerous regions of weak to transparent reflectivity. The crust-mantle boundary is clearly defined by a sharp decrease in reflectivity at the base of the lower crustal layer. Along the southern part of line 1 (Figure 3a), a lower crustal panel characterized by subhorizontal homogeneous reflectivity that underlies a region of heterogeneous, north dipping reflectivity in the southern part of the Wabigoon Subprovince correlates with a northward tapering anisotropic lower crustal layer inferred from the wide-angle reflection–refraction data [*Musacchio et al.*, 2004]. *White et al.* [2003] proposed that this layer represents an accreted Archean oceanic slab, and suggested the presence of a suture zone beneath the Wabigoon belt. A second suture was interpreted underneath the Uchi Subprovince, based on the presence of a crustal root characterized by north dipping reflectivity that appears to extend for a short distance into the upper mantle, and which truncates the subhorizontal lower crustal reflectivity observed in northern Uchi, Berens River and Sachigo subprovinces (Figure 3b). The presence of a crustal suture under the Uchi Subprovince was also suggested by *Calvert et al.* [2004] on the basis of reflection seismic data acquired 200 km to the west, along line 2b

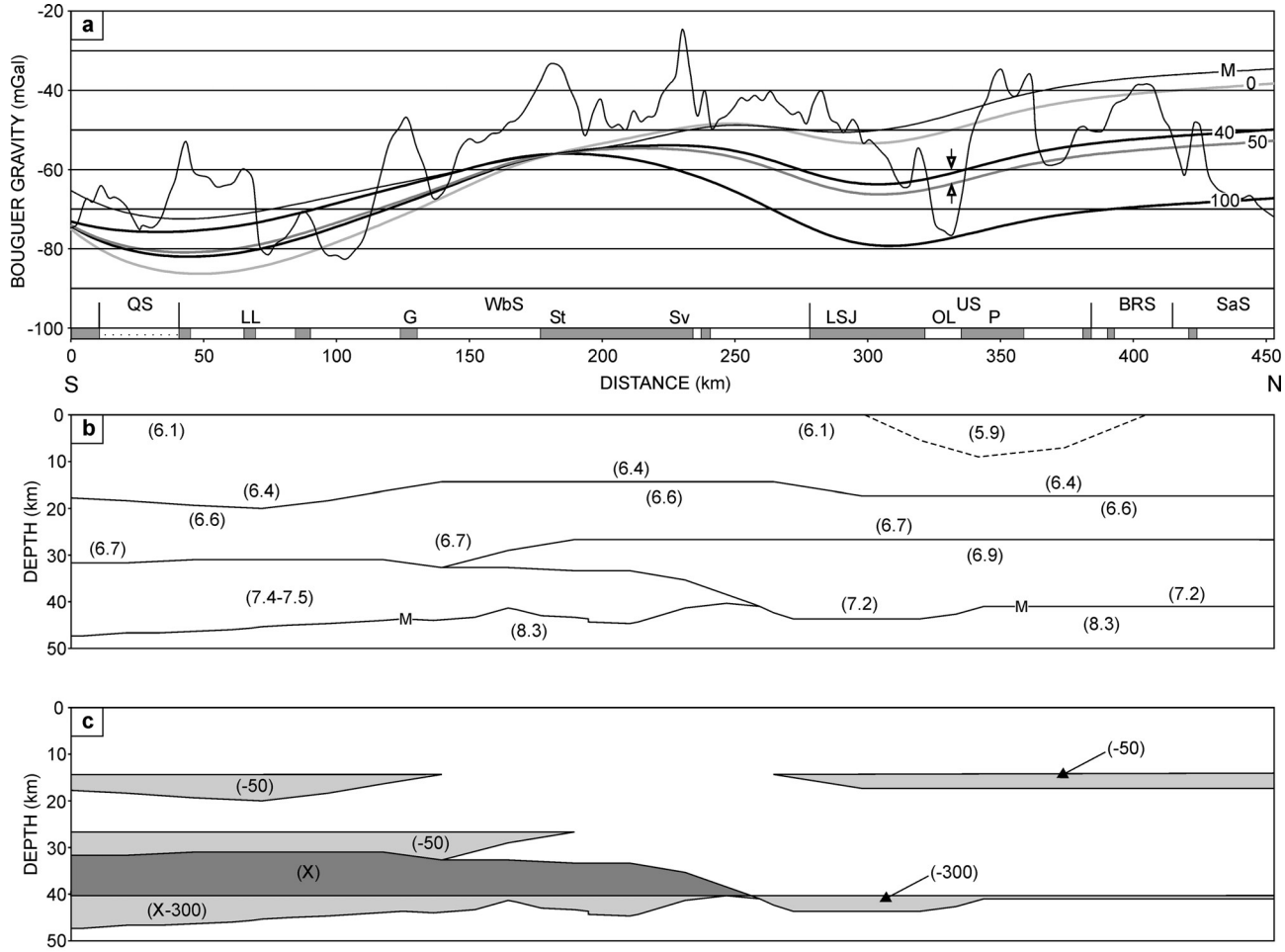

Figure 4. (a) Bouguer gravity field observed along the line 1 profile. Also shown are the calculated effect of the crust-mantle topography (labeled M) for a density contrast across this interface of 300 kg/m^3, as well as the calculated regional effect for different values (shown as labels) of the lateral density contrast assumed for the anisotropic lower crustal layer in the southern part of the profile. The calculated effects are plotted to reach the level inferred for the regional field (−56 mGal) at the point of maximum amplitude of the Sturgeon Lake gravity high. The arrows indicate the constrained range of possible levels of the regional field over the Ochig Lake pluton. The simplified surface lithology along the profile is indicated by a horizontal bar with shading and labels similar to those of Figure 1, and the boundaries between subprovinces are indicated by vertical segments. QS, Quetico Subprovince; WbS, Wabigoon Subprovince; US, Uchi Subprovince; BRS, Berens River Subprovince; SaS, Sachigo Subprovince. (b) Structure of the crust along the profile indicated by seismic data. The intracrustal boundaries correspond to the main velocity discontinuities inferred from wide-angle reflection–refraction data [*Musacchio et al.*, 2004]. The topography of the crust-mantle boundary is from near-vertical-incidence reflection data [*White et al.*, 2003]. In addition, a large upper crustal low-velocity region in the Uchi Subprovince is depicted with a dashed line. The P wave seismic velocities at various levels of the crustal layers are also shown (values in km/s). (c) Regions of lateral density contrast used in the calculation of the regional field. Lighter shading was applied to regions of negative lateral density contrast, and heavier shading was applied to regions of positive lateral density contrast. For each of these regions the lateral density contrast is indicated (values in kg/m^3). Several values of density contrast (X = 0, 40, 50, and 100 kg/m^3) were considered for the anisotropic lower crustal region in the southern part of the profile.

(Figure 3c), where, similar to line 1, a crustal root characterized by north dipping reflectivity is observed. In addition to accretion- or shortening-related reflection fabrics, the line 2b seismic section reveals several features (e.g., the upwarp of the crust-mantle boundary underneath the English River Subprovince; listric south dipping reflectors that extend into the lower crust from close to the surface contact between the Uchi and Berens River belts) that were previously inter-

preted as extensional structures [*Nitescu et al.*, 2003; *Calvert et al.*, 2004].

[12] The wide-angle reflection–refraction seismic data were collected along a north-south trending profile largely coincident with Lithoprobe seismic reflection line 1, and along an east-west trending profile crossing the northern part of the central Wabigoon Subprovince and the Winnipeg River Subprovince. The velocity models [*Musacchio et al.*, 2004] obtained from these data indicate a layered structure of the WS crust (Figure 4b), and reveal the presence under the Wawa, Quetico and central Wabigoon subprovinces of an anisotropic basal crustal layer characterized by P wave velocities of 7.4–7.5 and 6.9 km/s in the north-south and east-west directions, respectively. Along the regional strike, with respect to the north-south seismic line this layer appears to extend at least 50 km westward, and ~150–200 km eastward, under the Lake Nipigon region, where Mesoproterozoic mafic intrusive rocks crop out.

4. Forward Gravity Modeling

[13] In order to identify the major gravity anomaly sources at depth and to assess the relative contributions of shallow and deep sources to the WS gravity field (Figure 2), two-and-a-half-dimensional forward gravity modeling was carried out for the gravity data collected along Lithoprobe seismic lines 1 and 2b (Figure 1), which cross perpendicularly or at high angle the regional belt pattern of the WS, as well as the major topographic features of the crust-mantle boundary [see *Nitescu et al.*, 2003, Figure 8]. The actual gravity profiles were obtained by projecting the positions of the gravity stations on the N-S direction. A commercial two-and-a-half-dimensional potential field modeling software package (MAGIX; Interpex Ltd., Colorado) was used for the interpretation of the observed gravity anomalies, which were assumed to represent effects of horizontal prismatic bodies of finite E-W strike length. At surface, where there is relatively good control of the density distribution, the values of density contrast attributed to shallow structures were considered with respect to a density of 2690 kg/m^3, which is the mean density of exposed gneissic and tonalitic-trondhjemitic-granodioritic rocks in the region of study, and is believed to be representative for the upper part of the crust [e.g., *Gupta and Wadge*, 1986; *Szewczyk*, 1974]. For structures at depth the values of density contrast were selected on the basis of previous studies and (or) velocity-density relationships. In the case of the crust-mantle boundary, a constant density contrast of 300 kg/m^3 was assumed along seismic line 2b and north of the region of anisotropic lower crust observed along seismic line 1. This value is consistent with the density contrast values obtained from the conversion into densities of the P wave velocities recorded at the base of the crust (~7.1–7.2 km/s) and in the upper mantle (~8.3 km/s) using several empirical relationships (Table 1), as well as with the density contrast inferred from the average compositions of the lower crust and upper mantle of the shield lithosphere estimated by *Rudnik and Fountain* [1995]. For the segment of the line 1 gravity profile that corresponds to the region underlain by the layer of anisotropic lower crust, the value of the crust-mantle density contrast is dependent on the assumed lateral density contrast between this lower crustal layer and the rest of the lower crust (see next section). Along both gravity profiles the geometry of the crust-mantle boundary was constrained by seismic near-vertical-incidence reflection data. The strike extent considered on each side of the profiles for exposed mass anomalies (e.g., greenstone belts, granitoid plutons), as well as for the sources of the English River and Winnipeg River gravity anomalies was established based on the extent of their corresponding gravity effects. The topographic features of the Moho, as well as the deep intracrustal mass anomalies (i.e., depressions of the intracrustal boundaries and the region of anisotropic lower crust), were modeled assuming strike extents of 100 km on each side of the profiles. Although some of these features may have larger lateral extents [*Nitescu et al.*, 2003], the value we considered for their strike extent leads to realistic modeled gravity effects, since no significant difference in the calculated effects is obtained for larger values of strike extent.

Table 1. Values of Density Contrast Predicted by Various Density-Velocity Relationships

Seismic Discontinuity, km/s	Density Contrast, kg/m^3		
	Christensen and Mooney [1995]	*Yegorova et al.* [1997]	*Barton* [1986]
5.9–6.1	60[a]	60	60
6.4–6.6	50[b]	50	60
6.7–6.9	60[c]	50	60
7.2–8.3	280[d]	300	-

[a]Based on linear relationship for a depth of 10 km.
[b]Based on linear relationship for a depth of 20 km.
[c]Based on linear relationship for a depth of 30 km.
[d]Based on nonlinear relationship for a depth of 40 km.

4.1. Line 1 Profile

[14] The Bouguer gravity field along the line 1 profile, which extends in the north-south direction for about 450 km, has numerous anomalies with wavelengths smaller than 50 km that are superimposed on a component of the field characterized by wavelengths in the range 100–150 km (Figure 4a). The spatial correlations observed between the smaller-wavelength anomalies and the surface geology clearly demonstrate that most of these anomalies are related to surface density variations, which is also confirmed by previous local investigations, as well as by the data contained in an extensive density database of the WS (Geological Survey of Canada, unpublished data, 2001). There are only a few anomalies that are not related to surface variations in density (e.g., the along-strike continuation of the English River gravity high north of the Savant Lake greenstone belt; the gravity high in the Berens River Subprovince), but given their relatively small wavelengths, they are likely caused by density variations in the upper crust.

[15] The long-wavelength anomalies of the Bouguer gravity field appear to represent a "regional" component produced by density variations at depth. It can be observed

(Figure 4a) that this component of the field is characterized by a broad low in the southern part of the profile, an equally broad high in the central region of the profile, which corresponds to the northern part of the Wabigoon Subprovince, and an apparently smaller-amplitude low in the Uchi Subprovince. The character of the regional field in the Berens River and southern Sachigo subprovinces is not clear. Although the general trend of the regional field is relatively well indicated by the gravity data along most of the profile, its position with respect to the superimposed upper crustal gravity effects can be determined only if the magnitude of some of these effects can be independently estimated.

[16] Along the considered gravity profile, the level of the regional gravity field can be constrained on the basis of independent data at two locations. One of these is the Sturgeon Lake greenstone belt (St in Figures 1 and 4a), where previous gravity and high-resolution seismic investigations [*Dusanowskyj*, 1976; *Nedimovic*, 2000] indicate that the associated gravity high is related to a synform-shaped, 3-km-thick body of metavolcanic rocks characterized by a bulk density of $\sim$2950 kg/m^3. By using these source parameters to model the Sturgeon Lake gravity anomaly, we inferred that its maximum amplitude is of 22–23 mGal, which constrains the level of the regional field at the point where this gravity high reaches maximum amplitude to about −56 mGal (Figure 4a).

[17] A second location where the level of the regional gravity field can be estimated is in the region of the Ochig Lake pluton, at the southern boundary of the Pickle Lake greenstone belt (OL in Figures 1 and 4a). The amplitude of the Ochig Lake gravity low was constrained on the basis of information regarding its source geometry provided by the Lithoprobe wide-angle reflection – refraction data [*Musacchio et al.*, 2004], which indicate the occurrence in the upper crust of the Uchi Subprovince of a $\sim$9-km-deep synformal low-velocity zone characterized by a P wave velocity of 5.9 km/s (Figure 4b). This zone of lower seismic velocity correlates spatially with a major synformal region of transparent reflectivity observed in the upper crust of the northern Uchi Subprovince (Figure 3b), as well as with the occurrence of low-density granitoids at surface, and therefore is likely related to a large batholithic body of lower density. The spatial extent of this batholith as suggested by the seismic observations implies that it comprises both the Lake St. Joseph batholith and the Ochig Lake pluton, and underlies the Pickle Lake greenstone belt, extending to the granitoid region to the north (Figure 1). Therefore the Ochig Lake gravity low, which appears as a separate anomaly, is in fact part of a wider gravity low on which are superimposed the gravity highs related to the Pickle Lake greenstone belt and the smaller belt of metavolcanic rocks separating the Lake St. Joseph batholith and the Ochig Lake pluton (Figure 1). In a detailed gravity study of the western Uchi Subprovince, *Gupta and Wadge* [1986] have shown that the gravity lows observed west of the Meen-Dempster greenstone belt (MD in Figure 1) are related to granitoid plutons characterized by a negative density contrast of 50–60 kg/m^3 with respect to the assumed background density of 2690 kg/m^3. Such values of density contrast are likely representative for the low-velocity zone imaged in the region surrounding the Pickle Lake greenstone belt, being consistent with both the few density determinations available for the granitoid rocks in this region (Geological Survey of Canada, unpublished data, 2001), and the density contrast predicted from density-velocity relationships for the observed P wave velocities (Table 1). From the calculation of the gravity effect of this low-velocity zone for a negative density contrast of 50–60 kg/m^3 we obtained that at the point where the Ochig Lake gravity anomaly is largest, its amplitude reaches 13–16 mGal, which implies a level of the regional field in the range −60 to −63 mGal at this point (Figure 4). This conclusion is confirmed by the study of *Nitescu et al.* [2003], which, on the basis of the inversion of the long-wavelength components of the gravity field related to deep sources, suggests that the gravity low associated with the Ochig Lake pluton has an amplitude of $\sim$13 mGal [see *Nitescu et al.*, 2003, Figure 10].

[18] To investigate the main sources of the regional field, we calculated the gravity effects of the major crustal structures at depth (Figure 4), as indicated by the wide-angle reflection–refraction seismic data, with the exception of the crust-mantle interface topography, which was considered from the near-vertical incidence reflection data, where it is imaged with greater detail. The effect of the crust-mantle boundary topography (curve M in Figure 4a) reflects well the morphology of the regional field but fails to satisfy simultaneously both constraints previously discussed for the level of the regional field. This implies the existence of additional mass anomalies that contribute to the regional field. Such mass anomalies are probably related to the topography of the main intracrustal velocity discontinuities [*Musacchio et al.*, 2004], as is suggested by the correlation of their morphology with that of the regional field (Figure 4). A mass anomaly might also be associated with the region of anisotropic lower crust in the southern part of the profile, but the existence, as well as the nature of a gravity effect related to such a mass anomaly cannot be inferred solely from the qualitative inspection of the observed gravity data.

[19] The calculation of the gravity effects produced by the topography of intracrustal boundaries requires the estimation of the density contrasts associated with these interfaces. On the basis of several different empirical velocity-density relationships proposed for the crystalline crust [*Barton*, 1986; *Christensen and Mooney*, 1995; *Yegorova et al.*, 1997], the density increase predicted across these interfaces is on the order of 50 kg/m^3 (Table 1). Since in the case of the region of anisotropic lower crust in the southern part of the profile the velocity anisotropy makes the conversion to density uncertain, we calculated the regional field for several values of the density contrast of this region relative to the lower crustal layer north of it (curves 0, 40, 50, 100 in Figure 4a). The modeling results (Figure 4a) clearly indicate that the anomalies of the regional gravity field reflect the gravity effects of the topography of the crust-mantle and intracrustal interfaces, as well as a significant contribution from the anisotropic lower crustal layer in the southern part of the profile, which appears to be denser by

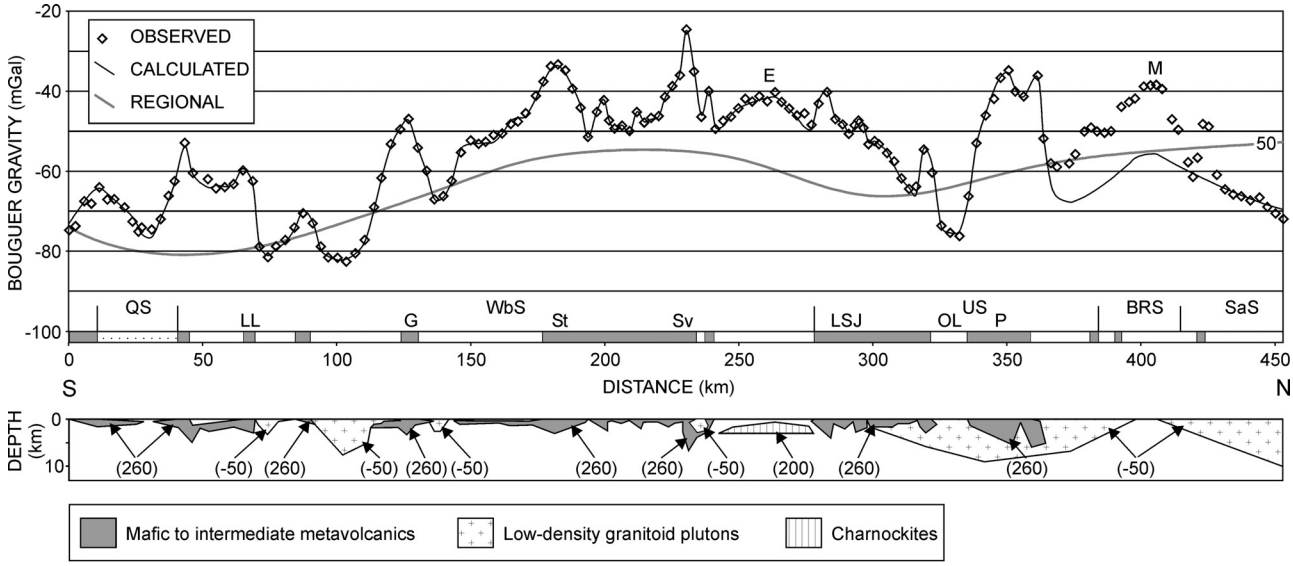

Figure 5. Two-and-a-half-dimensional gravity model of the upper crustal structures along line 1 profile. The value of density contrast assigned to each body is indicated (values in kg/m^3). The values of density contrast are with respect to a density of 2690 kg/m^3. The regional field corresponds to a lateral density contrast of 50 kg/m^3 for the anisotropic lower crustal layer in the southern part of the profile. The simplified surface lithology along the profile is indicated by a horizontal bar with shading and labels similar to those of Figure 1, and the boundaries between subprovinces are indicated by vertical segments. QS, Quetico Subprovince; WbS, Wabigoon Subprovince; US, Uchi Subprovince; BRS, Berens River Subprovince; SaS, Sachigo Subprovince.

$\sim$40–50 kg/m^3 than the lower crust north of it, based on the constraints inferred for the position of the regional field.

[20] The interpretation of the gravity effects related to upper crustal structures is presented in Figure 5. On the basis of previous density determinations [e.g., *Mackidd*, 1973; *Dusanowskyj*, 1976; *Gupta and Wadge*, 1986; Geological Survey of Canada, unpublished data, 2001], a density contrast of 260 kg/m^3 was assigned to the greenstone belt bodies, which are dominated in the region of the profile by mafic to intermediate metavolcanics, while for the granitic-granodioritic plutons associated with gravity lows a density contrast of -50 kg/m^3 was considered representative. It can be observed that most of the greenstone belts do not require depths beyond 1–3 km, with the exception of some cases where they require keels extending to 5–6 km (e.g., Savant Lake and Pickle Lake greenstone belts). Their relatively small depth extent and their inferred geometry are typical for such structures, which usually are less than 10 km deep, and have irregular bases [e.g., *Kusky and Vearncombe*, 1997]. There are only a few low-density plutonic bodies crossed by the gravity profile. In the northern part of the profile, in addition to the $\sim$9-km-thick batholith indicated by seismic data in the Uchi Subprovince (Figure 4b), an even thicker granitoid body ($\sim$10 km) is suggested by a large gravity low in the Sachigo Subprovince. The existence of such a large low-density body in the Sachigo belt is consistent with the partial imaging of an upper crustal low-velocity zone at the northern end of the velocity model presented by *Musacchio et al.* [2004]. In the Wabigoon Subprovince the low-density plutons crossed by the profile have smaller depths and horizontal extents compared to those observed in the Uchi and Sachigo subprovinces.

[21] In the case of the gravity high observed in the region underlain by granitoid rocks between the Savant Lake and Lake St. Joseph greenstone belts (E in Figure 5), since it forms a link between the prominent gravity anomaly observed in the western English River Subprovince and a similar anomaly in the eastern part of the subprovince (Figure 2), we interpreted its cause as related to that of the English River gravity high. Therefore this anomaly was modeled with a body of cross-sectional geometry, density contrast and depth similar to those suggested by *Nitescu et al.* [2006] for the source of the English River Subprovince gravity anomaly, which is considered by these authors to consist of dense charnockitic rocks.

[22] A gravity high of uncertain origin is observed in the Berens River Subprovince (M in Figures 2 and 5), in a region underlain by low-density granitic rocks (Geological Survey of Canada, unpublished data, 2001). Since there is no independent constraint for the nature and the characteristics of its source, this anomaly was not modeled. The occurrence of a narrow belt of dense metavolcanic rocks in its vicinity suggests, however, the possibility that it may be the effect of a greenstone belt covered by a granitic intrusion.

4.2. Line 2b Profile

[23] Along the line 2b gravity profile distinct gravity highs and lows with wavelengths smaller than 50 km are superimposed on a regional trend that appears characterized

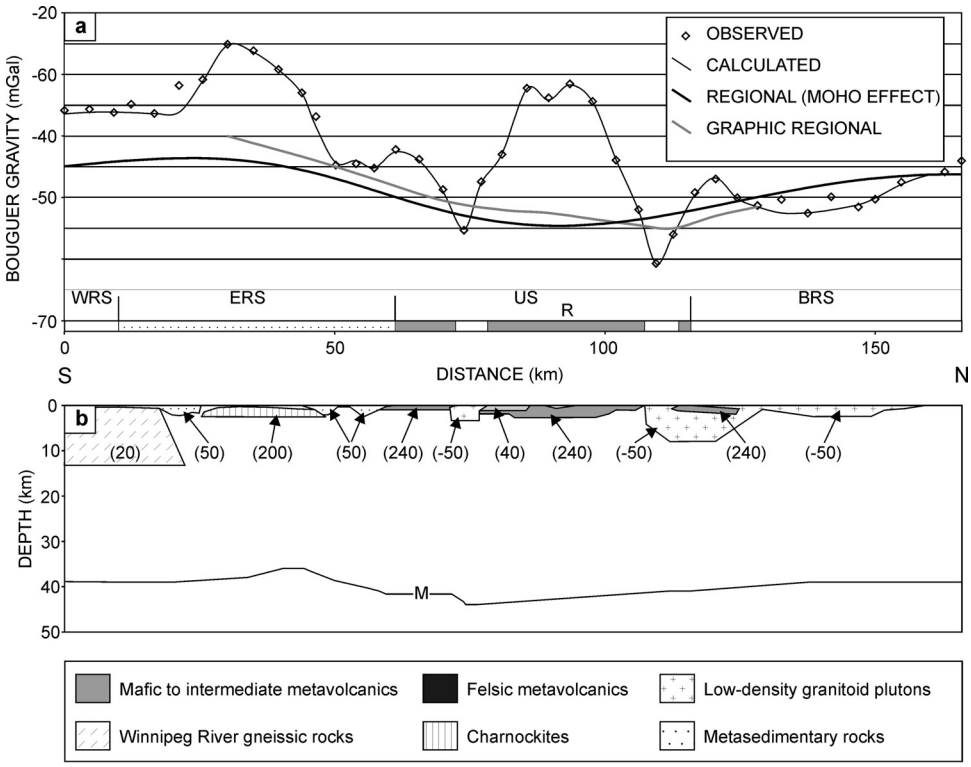

Figure 6. (a) Bouguer gravity field observed along the line 2b profile. The graphically separated regional field of *Gupta and Wadge* [1986], the calculated effect of the seismically determined crust-mantle topography, and the calculated Bouguer gravity obtained from the modeling of the residual anomalies (assuming as the regional field the gravity effect of the crust-mantle boundary) are also shown. The simplified surface lithology along the profile is indicated by a horizontal bar with shading and labels similar to those in Figure 1, and the boundaries between subprovinces are indicated by vertical segments. WRS, Winnipeg River Subprovince; ERS, English River Subprovince; US, Uchi Subprovince; BRS, Berens River Subprovince. (b) Two-and-a-half-dimensional gravity model of the upper crustal mass anomalies along line 2b profile. The value of density contrast assigned to each body is indicated (values in kg/m^3). The values of density contrast are with respect to a density of 2690 kg/m^3.The crust-mantle interface as inferred from near-vertical incidence reflection data is also shown (labeled M).

by a broad gravity high in the Winnipeg River and English River subprovinces, a gravity low in the Uchi Subprovince, and another gravity high in the Berens River Subprovince (Figure 6a). The morphology of the regional field is indicated by the graphically separated regional component of the gravity field (Figure 6a) that was obtained by *Gupta and Wadge* [1986]. It can be observed that the calculated gravity effect of the crust-mantle topography, as revealed by the near-vertical-reflection seismic data, matches well the morphology of the regional component obtained from graphical separation. The graphically separated regional effect shows amplitudes larger by up to 3–4 mGal for the regional anomalies in the English River Subprovince and in northern Uchi Subprovince, in an area of low-density granitic rocks, compared to the calculated effect of the crust-mantle interface, but this difference is likely due to small errors associated with the process of graphical separation of superimposed gravity effects of similar signs, as is the case at both of these locations. It appears therefore likely that the regional gravity field in the region of the WS crossed by Lithoprobe line 2b is mainly related to the topography of the crust-mantle boundary.

[24] The spatial correlation observed between the residual gravity effects that occur along the gravity profile in the Berens River and Uchi subprovinces and the exposed geological structures (Figure 6a), as well as the surface density of these structures [*Gupta and Wadge*, 1986], indicate that the gravity highs are produced by dense bodies of metavolcanic rocks, while the gravity lows relate to low-density granitic to granodioritic plutons. For the modeling of these residual anomalies, on the basis of the detailed density investigation carried out in the region by *Gupta and Wadge* [1986], we have assigned density contrast values of 240, 40 and −50 kg/m^3 to the bodies of mafic metavolcanic rocks, felsic metavocanics, and granitoid rocks, respectively, that correlate with the observed residual gravity effects. The results of gravity modeling (Figure 6b) suggest that a large low-density granitoid pluton straddles the boundary between the Uchi and Berens River subprovinces and reaches a depth of ~8 km, which is consistent with the observation

of a ~3-s-deep zone of transparent reflectivity in this region on the line 2b seismic section (Figure 3c). The modeling results also show that the large gravity high associated with the Red Lake greenstone belt is consistent with a 3-km-thick body of mafic metavolcanic rocks. For the modeling of the large residual gravity high observed in the English River Subprovince, which is considered to represent the effect of a dense charnockitic unit within a suite of shallow tonalitic plutons that intrude the English River metasediments [*Nitescu et al.*, 2006], we assumed a source of cross-sectional geometry, depth and density contrast similar to those suggested by *Nitescu et al.* [2006]. In addition, the gravity contributions of the thicker packages of metasediments (up to 2 km thick) that flank this intrusion, and which were interpreted on the basis of magnetic and seismic data [*Nitescu et al.*, 2006], were also considered.

[25] The main uncertainty in the interpretation of the gravity field along the line 2b profile concerns the source of the high gravity values in the Winnipeg River Subprovince, since this gravity effect does not correlate with an occurrence of denser rocks at surface, and the nature and characteristics of its source are not well constrained from other types of geophysical information. As previously discussed, it appears on the basis of seismic evidence that this gravity anomaly might be related to the presence of rocks from deep upper crustal and even midcrustal levels at a relatively elevated position, with respect to the neighboring terrains. Therefore we modeled the Winnipeg River gravity anomaly as the effect of a denser upper crustal layer characterized by a positive lateral density contrast of 20 kg/m^3, on the basis of the average density of tonalitic gneisses (2710 kg/m^3 [e.g., *Gupta and Barlow*, 1984]) that crop out at various locations in the Winnipeg River Subprovince, and which are considered representative for deeper upper crustal to midcrustal rocks.

5. Inverse Gravity Modeling

[26] The regional extent of the major mass anomalies that occur at depth in the study area was assessed by using density distributions determined with a three-dimensional gravity inversion algorithm (GRAV3D [*Li and Oldenburg*, 1998]). This algorithm approaches the inversion of gravity data as an optimization problem, by searching a density model that simultaneously minimizes an objective function of density and generates synthetic data matching the observations within a predetermined range of misfit. The objective function of density used by the GRAV3D algorithm provides the possibility of constraining the density model to be as close to a reference density model as possible, consistent with fitting the data, thereby allowing the incorporation of additional information into the inversion (e.g., the density contrast and spatial distribution of known mass anomalies [*Li and Oldenburg*, 1998]). An important feature of the objective function is a depth weighting factor that prevents the concentration of the modeled density anomalies at surface, regardless of the true depth of the gravity anomaly sources, because of the inherent lack of depth resolution of gravity data. Using this inversion procedure, model roughness that is not required to fit the data is suppressed. The numerical solution to the inverse problem is obtained by discretizing the subsurface volume that contains the gravity anomaly sources into a large number of rectangular cells, which are assumed to have constant density.

[27] Because of the conditions of spatial smoothness and of closeness to the reference model imposed by the inversion algorithm, the density model that would be recovered from the unconstrained inversion (i.e., using a zero-density contrast reference density model) of the gravity data set would contain mass anomalies having a significantly larger vertical extent, but smaller density contrast values than the real structures that account for the observed gravity effects. In such a case, the sources that model upper crustal gravity anomalies could extend to middle and even lower crustal levels, masking the distribution of deeper regions of density contrast and precluding their identification.

[28] To eliminate this effect, the gravity inversion was constrained by incorporating into the reference density model descriptions of the main upper crustal mass anomalies that approximate their volume and density contrast, based on available geological and geophysical information (Figure 7). For all the considered upper crustal structures, it was assumed that they are composed of vertical prisms, and their lateral extent was approximated on the basis of the extent of their corresponding gravity effects. The greenstone belt bodies and the low-density granitoid plutons were assigned values of density contrast of 250 and -50 kg/m^3, respectively, and were all assumed initially to have depth extents of 3 and 5 km, respectively, which are representative values of density contrast and depth extent for such structures in the WS. However, it was observed that the inversion of the gravity data using this initial reference model would produce density distributions characterized by significant tails at depth for some of the upper crustal mass anomalies in the Wabigoon Subprovince, and therefore the depth extents of those mass anomalies in the reference density model were subsequently adjusted to 5 km in the case of greenstone belts and to 10 km in the case of low-density granitoid bodies. For the source of the English River gravity anomaly, it was assumed that it has a density contrast of 200 kg/m^3 and that it extends between 1 and 3 km depth, based on its characteristics inferred by *Nitescu et al.* [2006]. In the case of the source of the Winnipeg River anomaly we assumed, consistent with the forward gravity model obtained along Lithoprobe line 2b (Figure 6), that it is produced by a 10-km-thick upper crustal layer characterized by a positive density contrast of 20 kg/m^3.

[29] We have applied the inversion algorithm to the residual field obtained by subtracting from the WS gravity field (Figure 2) the gravity effect corresponding to the model of the Moho topography presented by *Nitescu et al.* [2003]. The recovered density model (Figure 8) indicates a prominent positive mass anomaly at midcrustal and lower crustal depths in the southeastern region of the study area. We correlate this mass anomaly with the northern segment of the slab of denser and seismically anisotropic lower crust that occurs in the southeastern part of the area of investigation [*Musacchio et al.*, 2004], this correlation being also

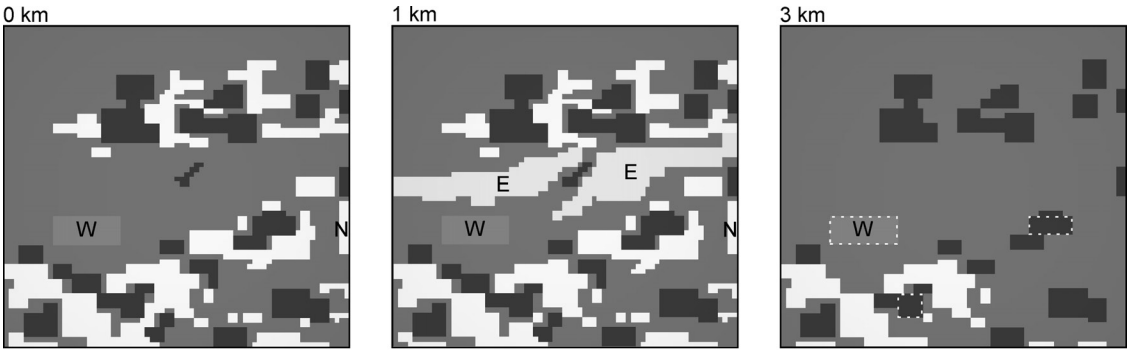

Figure 7. Reference density model. Approximations of the main upper crustal mass anomalies were incorporated as shown in horizontal depth slices from three upper crustal levels. The unlabeled white structures correspond to greenstone belts and have a density contrast of 250 kg/m^3. The black structures correspond to low-density plutons and have a density contrast of −50 kg/m^3. The structure labeled E corresponds to the source of the English River gravity anomaly and has a density contrast of 200 kg/m^3. The structure labeled W corresponds to the source of the Winnipeg River gravity anomaly and has a density contrast of 20 kg/m^3. The structure labeled N represents a shallow westward extension of Mesoproterozoic mafic intrusive rocks exposed in Lake Nipigon region and has a density contrast of 290 kg/m^3. The structures surrounded with dotted lines in the 3 km depth slice extend to a depth of 10 km. All the other structures shown in the 3 km depth slice extend to a depth of 5 km. In the horizontal plane the reference density model corresponds to a rectangular region having 355 km along the east-west direction and 330 km along the north-south direction.

supported by the occurrence of peak values of density contrast at lower crustal depths (see vertical section AA′ in Figure 8). The inversion model also indicates that this mass anomaly is continued toward the southwest by an elongated distribution of positive density contrast, which likely defines the westward extent of the slab of denser lower crust (Figure 8). The occurrence of a small region of negative density contrast to the south-southeast of this elongated distribution of positive density contrast (see arrow plotted on the 30 km depth slice in Figure 8) likely reflects the area where negative gravity effects corresponding to depressions of the interfaces between the main crustal layers offset the positive gravity contribution of the slab of denser lower crust. It is noticed, however, that the deep mass anomalies recovered in the inversion model have larger vertical extent, but smaller density contrast values compared to their vertical extent and density contrast inferred from seismic data and gravity forward modeling, respectively. As previously discussed, this represents the effect of the constraints imposed on the solution by the inversion algorithm.

6. Discussion

[30] The results obtained from forward modeling of the WS gravity data suggest that with the exception of the southeastern region of the area of investigation (Figure 1), significant mass anomalies occur only in the upper crust and at the crust-mantle boundary. The gravity models show that the upper crustal density heterogeneities extend within the first 10 km of the crust, and suggest the absence of important lithological contrasts at larger depths, both within and between the different WS subprovinces.

[31] The remarkable lateral uniformity of the density stratification inferred from gravity modeling for the mid-crustal and lower crustal levels is unlikely to have resulted solely from the accretion of similarly stratified arc and continental fragments. It is more plausible that the absence of mass anomalies at deep crustal levels is related to postaccretionary reorganization of the crustal density structure. The occurrence of mass redistribution processes that would account for such a reorganization may have been the effect of a major episode of intracrustal softening and crustal differentiation, which is indicated by voluminous late orogenic granitic magmatism in the interval 2.71–2.66 Ga. The thermal perturbation responsible for this softening episode has been attributed to thermal blanketing produced by a thick cover of volcanics [*West and Mareschal*, 1979], to crustal thickening [e.g., *Williams et al.*, 1992; *Card and Poulsen*, 1998], and more recently, to the combined thermal effects produced by a thick greenstone layer and a mantle plume [*Rey et al.*, 2003]. Regardless of the exact origin of the thermal anomaly, it is reasonable to assume that thermal softening of the crust led to the elimination of preexistent intracrustal mass anomalies at deeper levels of the crust through processes of gravitational segregation and ductile lateral flow. The former processes may have included not only the transfer and emplacement at high crustal levels of low-density felsic material extracted from partially molten midcrustal to lower crustal rocks, but also the foundering of mafic intrusions initially emplaced at levels subsequently affected by thermal softening [e.g., *Glazner*, 1994; *Bailey and Pearse*, 2004]. Moreover, if the crust was indeed blanketed by a thick (6–12 km) layer of volcanics [*West and Mareschal*, 1979; *Rey et al.*, 2003], then the small depth extents of the WS greenstone belts (less than 5 km) and the

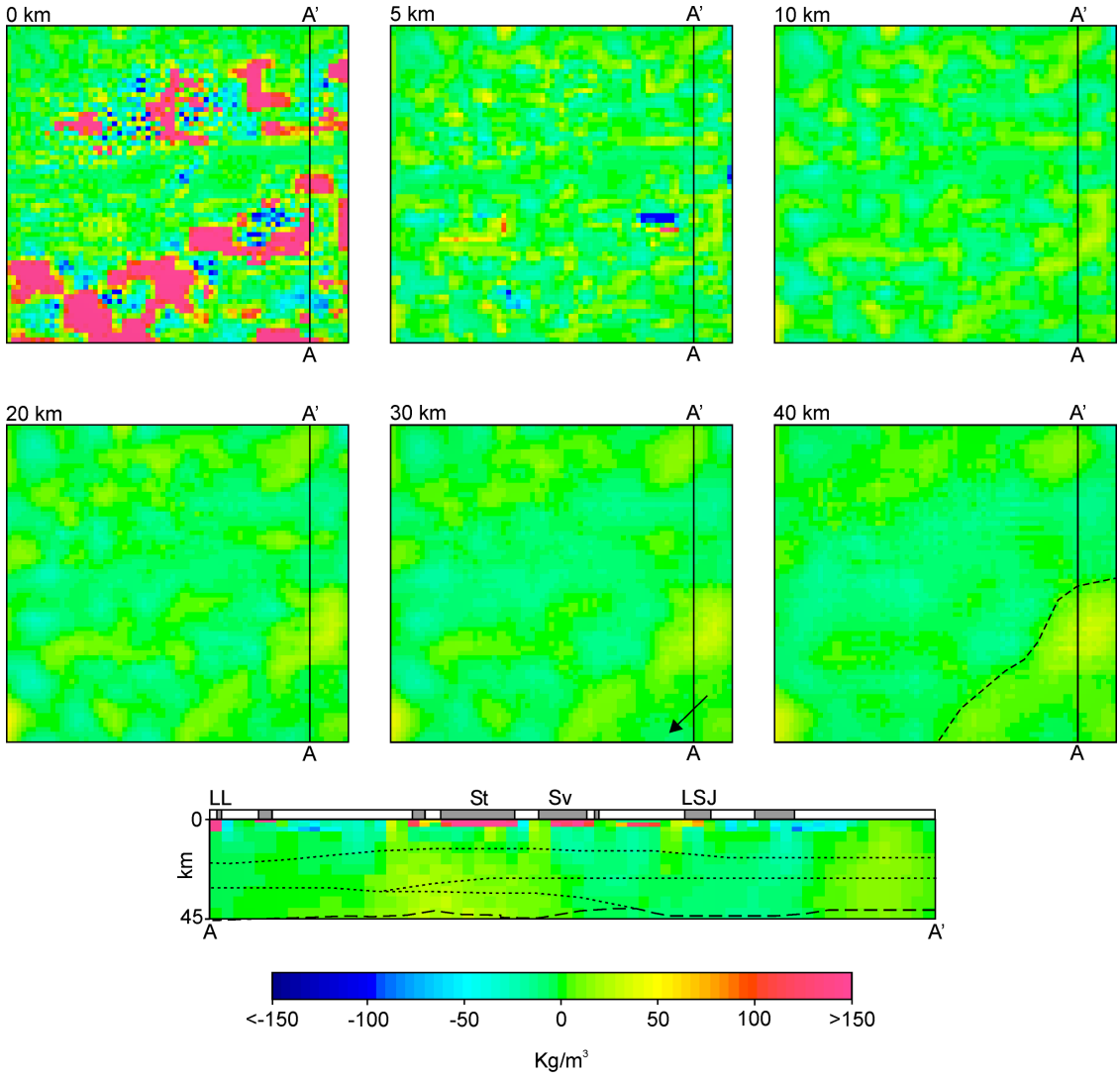

Figure 8. Density model recovered from the inversion of the residual gravity field (i.e., the field obtained through the subtraction from the Bouguer gravity field of the gravity effect produced by the crust-mantle interface topography) for the case when constraints for the main upper crustal gravity sources were incorporated into the reference density model (Figure 7). The model is shown in horizontal depth slices from six depth levels and in a north trending vertical section (AA′), which approximately coincides with the position of line 1 seismic profile. The density model corresponds to a subsurface volume that has 355 km along the east-west direction and 330 km along the north-south direction and extends to a depth of 45 km. For the inversion of gravity data this volume was discretized in a mesh of rectangular cells that has 71 cells in the easting direction, 66 cells in the northing direction, and 11 cells in thickness. The size of cells is 5 km in both the easting and northing direction. In the depth direction the first three layers of cells from the surface have thicknesses of 1, 2, and 2 km, respectively, while the rest of the layers are 5 km thick. The horizontal depth slices and the vertical sections are shown at different scales. The vertical section is represented without any vertical exaggeration, and its position is indicated on each of the horizontal depth slices. The simplified surface lithology along section AA′ is indicated by a horizontal bar with shading and labels similar to those in Figure 1. The topography of the crust-mantle interface observed along seismic line 1 (dashed line), as well as the boundaries of the main crustal layers indicated by the wide-angle reflection–refraction data (dotted lines) were plotted on cross section AA′. The dashed line plotted on the 40 km depth slice shows the possible northwestern extent of the segment of denser lower crust that underlies the southeastern region of the study area. The arrow plotted on the 30 km depth slice indicates a negative mass anomaly that likely reflects the occurrence of depressions of the interfaces between the main crustal layers.

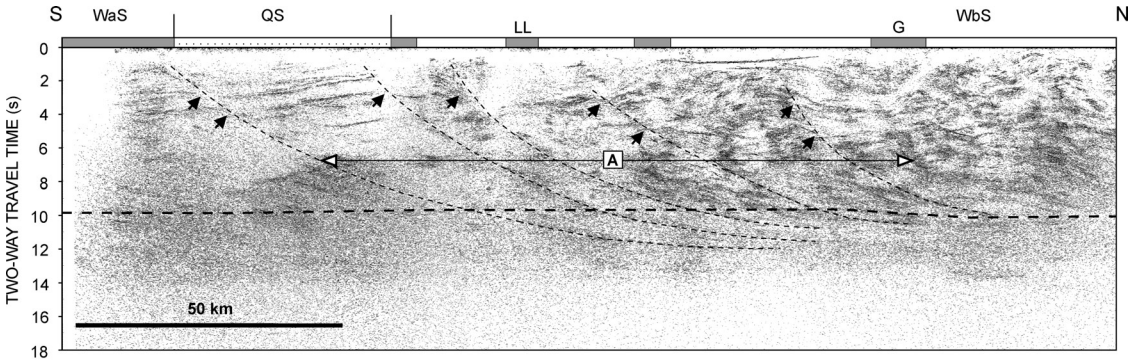

Figure 9. Enlarged segment of the Lithoprobe line 1 seismic section presented in Figure 3a, showing the seismic reflectivity observed in the Wawa Subprovince (WaS), Quetico Subprovince (QS), and southern part of the Wabigoon Subprovince (WbS). The simplified surface lithology along the profile is indicated by a horizontal bar with shading and labels similar to those of Figure 1, and the boundaries between subprovinces are indicated by vertical segments. The thick dashed line corresponds to the top of the anisotropic lower crustal layer revealed by the spatially coincident refraction–wide-angle reflection data. The horizontal arrowed line (A) indicates a midcrustal region where north dipping reflectors are observed. The thin dashed lines correspond to north dipping shear zones for which a normal sense of displacement is suggested by deflections of various reflectors they intersect. These deflections are indicated by black arrows.

absence in most cases of a stratigraphic contact of the greenstones with the underlying felsic basement suggest that part of the volcanic material was also transferred downward following the softening of the felsic basement. Ductile lateral flow probably explains the absence in most of the investigated area of significant topographic features at the interface between the middle and the lower crustal layers, which is a first-order seismic velocity discontinuity [*Musacchio et al.*, 2004], and likely represents also a density contrast boundary. The occurrence of late orogenic ductile extensional flow at deep crustal levels in the crust of the Superior Province was previously inferred on the basis of structural and geochronological information from an uplifted midcrustal block in the southern Superior Province (i.e., Wawa gneiss domain [*Moser et al.*, 1996]), and is consistent with the evolution of the deep crust observed in other orogens affected by thermal softening [e.g., *Vanderhaeghe and Teyssier*, 2001].

[32] The only major midcrustal and lower crustal mass anomalies inferred from the current gravity study occur in the southeastern part of the investigation area (Figure 1), which corresponds to the southern region of the central Wabigoon Subprovince. These mass anomalies are related to depressions of the interfaces between the main crustal layers, and to an underlying segment of seismically anisotropic lower crust [*Musacchio et al.*, 2004] characterized by larger bulk density relative to the lower crust north and west of it (Figure 4). On the basis of its seismic characteristics (i.e., velocity, V_P/V_S ratio, anisotropy), this lower crustal segment was interpreted by *White et al.* [2003] and *Musacchio et al.* [2004] as a metamorphosed oceanic slab accreted at the base of the continental crust during the final stages of the WS amalgamation. However, such an interpretation is not unequivocal, given (1) the apparently limited westward extent of the segment of denser lower crust, as indicated by the results of inverse gravity modeling (Figure 8), as well as by the wide-angle reflection–refraction data [*Musacchio et al.*, 2004], which would imply a significant variation in the subduction behavior of presumably the same oceanic slab under the Wabigoon terrain; (2) the limited lateral extent of seismic reflectivity possibly indicative of tectonic underplating, such as a midcrustal north dipping reflectivity package in the southern Wabigoon region (Figure 3a) that was previously interpreted as an accretionary imbricate stack formed in response to underthrusting [*White et al.*, 2003]; and (3) the vertical extent of this reflectivity package, which appears to sole within, and not at the top of the lower crustal layer, where the main thrust fault would be expected to occur (see also Figure 9).

[33] An alternative origin for the segment of dense and anisotropic lower crust observed underneath the Wawa, Quetico, and central Wabigoon subprovinces is the emplacement of mantle-derived mafic melts into and at the base of the lower crust. Such processes of magmatic intra and underplating are generally considered important for the growth and modification of the lower continental crust, and could explain the higher density and the different seismic characteristics (i.e., high seismic anisotropy, high seismic velocity) of the lower crust in the southeastern part of the study area [e.g., *Herzberg et al.*, 1983; *Furlong and Fountain*, 1986; *Fyfe*, 1992; *Holbrook et al.*, 1992]. *White et al.* [2003] and *Musacchio et al.* [2004] have indicated that the petrophysical characteristics (average P wave velocity, V_P/V_S ratio, density) of this lower crustal region are consistent with the composition of a troctolite, which is a plausible rock for a magmatic underplate [e.g., *Best*, 2003]. Although these authors have eventually preferred an alternative interpretation by suggesting an amphibolitic composition for this lower crustal region, which accounts easily for the observed high P wave anisotropy (~7%), the occurrence

of a rock of gabbroic composition characterized by such seismic anisotropy cannot be excluded in the case of high olivine content (>15%) and strong preferred orientation of the olivine crystals [e.g., *Christensen*, 1978]. A likely possibility is the formation of this lower crustal segment in relation to the circa 1.1 Ga plume-related Midcontinent (Keweenawan) rifting event, which may have affected a significant region of the WS lower crust through the emplacement of both upper mantle and mantle plume melts [e.g., *Allen et al.*, 1995]. This hypothesis is supported by (1) the occurrence of the Keweenawan rift margin only ~100 km south to southeast of the study area, and the southward thickening of this lower crustal layer; (2) the eastward extent of this layer under the Keweenawan intrusive rocks that crop out in the Lake Nipigon region [*Musacchio et al.*, 2004], which is thought to represent a failed arm of the Midcontinent rift [e.g., *Sutcliffe*, 1991]; (3) seismic and gravity models suggesting the presence beneath the axis of the rift in the Lake Superior region of a thick (>10 km), high-velocity (> 7 km/s), high-density lower crustal layer thought to have been formed through a combination of intra and underplating [e.g., *Trehu et al.*, 1991; *Mariano and Hinze*, 1994]; and (4) the occurrence of Keweenawan mafic dikes in the region of the Irene-Eltrut batholith of the Wabigoon Subprovince (IE in Figure 1), to the west of the inferred margin of the segment of anomalous lower crust (Figure 8), as well as in the Quetico and Wawa subprovinces, in the region crossed by Lithoprobe seismic line 1 [*Ontario Geological Survey*, 1991], which suggests that Keweenawan magmatism may have extended at depth beyond the areas of its upper crustal manifestation (i.e., the northwestern shore of Lake Superior and the Lake Nipigon region). In addition, this hypothesis is consistent with the interpretation of *Allen et al.* [1992] of the occurrence of both a regional topographic dome and a regional gravity low centered on Lake Superior as a consequence of the Keweenawan plume that is indicative of a broad region of underplated crust and (or) low-density depleted upper mantle extending several hundred kilometers beyond the margins of the rift.

[34] The extension of north dipping reflectors observed in the Quetico and southern Wabigoon subprovinces (see region A in Figure 9) into the lower crustal layer, where they become subhorizontal (Figure 9), suggests that this package of reflectivity postdates the formation or the emplacement of the segment of dense lower crust that underlies this region. In addition, it appears that this north dipping reflectivity corresponds to a set of normal shear zones, based on the deflection observed in the case of several reflectors (see arrows in Figure 9). We suggest that if the segment of denser lower crust that occurs in the central Wabigoon, Quetico, and Wawa subprovinces is related to the Keweenawan rifting event, then the observed set of north dipping normal shear zones formed in response to the extensional state of stress that must have prevailed in this segment of the crust at circa 1.1 Ga, as a result of lithospheric uplift produced by plume impingement in the Lake Superior region. We also speculate that normal movement on this set of shear zones might explain the large depression of the interface between the upper crustal and middle crustal layers that is indicated by the velocity model in this region (Figure 4b), and which accounts for an important negative gravity effect.

7. Conclusions

[35] Results of forward modeling of gravity data along two profiles corresponding to major Lithoprobe seismic lines and from the three-dimensional inversion of regional gravity data provide a comprehensive perspective on the distribution of mass anomalies within the WS crust, leading to the following conclusions regarding the crustal structure and the evolution of the Western Superior craton:

[36] 1. Most of the WS crust is characterized by the absence of major intracrustal mass anomalies at midcrustal and lower crustal depths. Generally, significant mass anomalies occur at the crust-mantle boundary, where they are associated with undulations of this interface, and in the first 10 km of the crust, where they are represented mainly by greenstone belts and granitoid bodies.

[37] 2. The remarkable absence at midcrustal and lower crustal depths of a lateral density segmentation inherited from the accretionary or collisional stages of the WS evolution is consistent with the hypothesis that postaccretionary thermal softening reworked the deep levels of the WS crust through mass redistribution processes, such as vertical mass transfer and ductile extensional flow.

[38] 3. Major intracrustal mass anomalies are observed only in a region that extends from the central Wabigoon Subprovince southward. These mass anomalies correspond to a segment of denser and seismically anisotropic lower crust, and to depressions of the interfaces between the main crustal layers. On the basis of various geological and geophysical observations it appears that these structures may reflect postcratonization modifications related to the 1.1 Ga Keweenawan rifting event.

[39] **Acknowledgments.** We thank the University of British Columbia Geophysical Inversion Facility for providing an academic license of the GRAV3D program. We also thank C. Andronicos, A. Hynes, and G. Keller for constructive reviews. This is Lithoprobe contribution 1433.

References

Allen, D. J., W. J. Hinze, and W. F. Cannon (1992), Drainage, topographic, and gravity anomalies in the Lake Superior region: Evidence for a 1100 Ma mantle plume, *Geophys. Res. Lett.*, *19*, 2119–2122.

Allen, D. J., L. W. Braile, W. J. Hinze, and J. Mariano (1995), The Midcontinent Rift System, U.S.A.: A major Proterozoic continental rift, in *Continental Rifts: Evolution, Structure, Tectonics*, edited by K. H. Olsen, pp. 375–407, Elsevier, New York.

Bailey, R. C., and J. Pearse (2004), The surface geodynamic expression of ongoing density stratification in the heated continental crust, *Eos Trans. AGU*, *85*(17), Jt. Assem. Suppl., Abstract T21B-06.

Barton, P. J. (1986), The relationship between seismic velocity and density in the continental crust—A useful constraint?, *Geophys. J. R. Astron. Soc.*, *87*, 195–208.

Beakhouse, G. P. (1991), Winnipeg River Subprovince, in *Geology of Ontario*, edited by P. C. Thurston et al., pp. 279–301, Ont. Geol. Surv., Toronto, Canada.

Best, M. G. (2003), *Igneous and Metamorphic Petrology*, 2nd ed., 729 p., Blackwell Sci., Malden, Mass.

Brisbin, W. C., and A. G. Green (1980), Gravity model of the Aulneau batholith, northwestern Ontario, *Can. J. Earth Sci.*, *17*, 968–977.

Calvert, A. J., E. W. Sawyer, W. J. Davis, and J. N. Ludden (1995), Archean subduction inferred from seismic images of a mantle suture in the Superior Province, *Nature*, *375*, 670–674.

Calvert, A. J., A. R. Cruden, and A. Hynes (2004), Seismic evidence for preservation of the Archean Uchi granite-greenstone belt by crustal-scale extension, *Tectonophysics*, *388*, 135–143.

Card, K. D. (1990), A review of the Superior Province of the Canadian Shield, a product of Archean accretion, *Precambrian Res.*, *48*, 99–156.

Card, K. D., and A. Ciesielski (1986), Subdivisions of the Superior Province of the Canadian Shield, *Geosci. Can.*, *13*, 5–13.

Card, K. D., and K. H. Poulsen (1998), Geology and mineral deposits of the Superior Province of the Canadian Shield, in *Geology of Canada*, vol. 7, *Geology of the Precambrian Superior and Grenville Provinces and Precambrian Fossils in North America*, coordinated by S. B. Lucas and M. R. St-Onge, pp. 13–194, Geol. Surv. Can., Ottawa.

Christensen, N. I. (1978), Ophiolites, seismic velocities and oceanic crustal structure, *Tectonophysics*, *47*, 131–157.

Christensen, N. I., and W. D. Mooney (1995), Seismic velocity structure and composition of the continental crust: A global view, *J. Geophys. Res.*, *100*, 9761–9788.

Corfu, F. (1988), Differential response of U-Pb systems in coexisting accessory minerals, Winnipeg River Subprovince, Canadian Shield: Implications for Archean crustal growth and stabilization, *Contrib. Mineral. Petrol.*, *98*, 312–325.

Corfu, F., and D. Stone (1998), Age structure and orogenic significance of the Berens River composite batholiths, Western Superior Province, *Can. J. Earth Sci.*, *35*, 1089–1109.

Corfu, F., and G. M. Stott (1993), U-Pb geochronology of the central Uchi Subprovince, Superior Province, *Can. J. Earth Sci.*, *30*, 1179–1196.

Corfu, F., G. M. Stott, and F. W. Breaks (1995), U-Pb geochronology and evolution of the English River Subprovince, an Archean low P–high T metasedimentary belt in the Superior Province, *Tectonics*, *14*, 1220–1233.

Cruden, A. R., D. Davis, M. Melnyk, P.-Y. F. Robin, and T. Menard (1998), Structural and geochronological observations at Kenora: Implications for the style and timing of deformation during the Kenoran orogeny, NW Ontario, in *Western Superior Lithoprobe Transect Fourth Annual Workshop*, edited by R. M. Harrap and H. H. Helmstaedt, *Lithoprobe Rep. 65*, pp. 54–62, Lithoprobe Secr., Univ. of B. C., Vancouver, Canada.

Davis, D. W. (1998), Speculations on the formation and crustal structure of the Superior province from U-Pb geochronology, in *Western Superior Lithoprobe Transect Fourth Annual Workshop*, edited by R. M. Harrap and H. H. Helmstaedt, *Lithoprobe Rep. 65*, pp. 21–28, Lithoprobe Secr., Univ. of B. C., Vancouver, Canada.

Davis, D. W., F. Pezzutto, and R. J. Ojakangas (1990), The age and provenance of metasedimentary rocks in the Quetico Subprovince, Ontario from single zircon analyses: Implications for Archean sedimentation and tectonics in the Superior Province, *Earth Planet. Sci. Lett.*, *99*, 95–105.

Dentith, M. C., V. F. Dent, and B. J. Drummond (2000), Deep crustal structure in the southwestern Yilgarn Craton, Western Australia, *Tectonophysics*, *325*, 227–255.

Dusanowskyj, T. H. (1976), A gravity study of the Sturgeon Lake metavolcanic-metasedimentary belt, M.Sc. thesis, 75 pp., Univ. of Toronto, Toronto, Ont., Canada.

Furlong, K. P., and D. M. Fountain (1986), Continental crustal underplating: Thermal considerations and seismic-petrologic consequences, *J. Geophys. Res.*, *91*, 8285–8294.

Fyfe, W. S. (1992), Magma underplating of continental crust, *J. Volcanol. Geotherm. Res.*, *50*, 33–40.

Glazner, A. F. (1994), Foundering of mafic plutons and density stratification of continental crust, *Geology*, *22*, 435–438.

Gupta, V. K., and R. B. Barlow (1984), A detailed gravity profile across the English River Subprovince, northwestern Ontario, *Can. J. Earth Sci.*, *21*, 145–151.

Gupta, V. K., and D. R. Wadge (1986), Gravity study of the Birch, Uchi and Red Lakes area, District of Kenora (Patricia Portion), *Rep. 252*, 98 p., Ont. Geol. Surv., Toronto, Canada.

Hall, D. H., and Z. Hajnal (1969), Crustal structure of northwestern Ontario: Refraction seismology, *Can. J. Earth Sci.*, *6*, 82–99.

Hall, D. H., and Z. Hajnal (1973), Deep seismic studies in Manitoba, *Bull. Seismol. Soc. Am.*, *63*, 895–910.

Herzberg, C. T., W. S. Fyfe, and M. J. Carr (1983), Density constraints on the formation of the continental Moho and crust, *Contrib. Mineral. Petrol.*, *84*, 1–5.

Hoffman, P. F. (1989), Precambrian geology and tectonic history of North America, in *The Geology of North America*, vol. A, *The Geology of North America: An Overview*, edited by A. W. Bally and A. R. Palmer, pp. 447–512, Geol. Soc. of Am., Boulder, Colo.

Holbrook, W. S., W. D. Mooney, and N. I. Christensen (1992), The seismic velocity structure of the deep continental crust, in *Continental Lower Crust*, edited by D. M. Fountain, R. Arculus, and R. W. Kay, pp. 1–43, Elsevier, New York.

Krogh, T. E., N. B. W. Harris, and G. L. Davis (1976), Archean rocks from the eastern Lac Seul region of the English River Gneiss Belt, northwestern Ontario, part 2. Geochronology, *Can. J. Earth Sci.*, *13*, 1212–1215.

Kusky, T. M., and J. R. Vearncombe (1997), Structural aspects, in *Greenstone Velts*, edited by M. J. de Wit and L. D. Ashwal, pp. 91–124, Clarendon, Oxford, U.K.

Langford, G. F., and J. A. Morin (1976), The development of the Superior Province of northwestern Ontario by merging island arcs, *Am. J. Sci.*, *276*, 1023–1034.

Li, Y., and D. W. Oldenburg (1998), 3-D inversion of gravity data, *Geophysics*, *63*, 109–119.

Mackidd, D. G. (1973), Interpretation of gravity and magnetics north of Lake Superior, M.Sc. thesis, 103 pp., Univ. of Toronto, Toronto, Ont., Canada.

Mariano, J., and W. J. Hinze (1994), Gravity and magnetic models of the Midcontinent Rift in eastern Lake Superior, *Can. J. Earth Sci.*, *31*, 661–674.

Melnyk, M., D. W. Davis, A. R. Cruden, and R. A. Stern (2006), U-Pb ages of magmatism constraining regional deformation in the Winnipeg River Subprovince and Lake of the Woods greenstone belt: Evidence for Archean terrane accretion in the Western Superior Province, *Can. J. Earth Sci.*, in press.

Moser, D. E., L. M. Heaman, T. E. Krogh, and J. A. Hanes (1996), Intracrustal extension of an Archean orogen revealed using single-grain U-Pb zircon geochronology, *Tectonics*, *15*, 1093–1109.

Musacchio, G., D. J. White, I. Asudeh, and C. J. Thomson (2004), Lithospheric structure and composition of the Archean Western Superior Province from seismic refraction/wide-angle reflection and gravity modeling, *J. Geophys. Res.*, *109*, B03304, doi:10.1029/2003JB002427.

Nedimovic, M. R. (2000), Seismic reflection imaging in crystalline terrains, Ph.D. thesis, 185 pp., Univ. of Toronto, Toronto, Ont., Canada.

Nitescu, B., and A. R. Cruden (2001), Gravity models of the English River Subprovince: Implications for its deep structure and tectonic origin, in *Western Superior Lithoprobe Transect Seventh Annual Workshop*, edited by R. M. Harrap and H. H. Helmstaedt, *Lithoprobe Rep. 80*, pp. 136–141, Lithoprobe Secr., Univ. of B. C., Vancouver, Canada.

Nitescu, B., A. R. Cruden, and R. C. Bailey (2003), Topography of the crust-mantle interface under the Western Superior craton from gravity data, *Can. J. Earth Sci.*, *40*, 1307–1320.

Nitescu, B., A. R. Cruden, and R. C. Bailey (2006), Integrated potential-field and seismic constraints on the structure of the Archean metasedimentary English River belt, Western Superior craton, Canada, *Precambrian Res.*, *144*, 261–277.

Ontario Geological Survey (1991), Bedrock geology of Ontario, west-central sheet, *Map 2542*, Ont. Geol. Surv., Sudbury, Canada.

Rey, P. F., P. Philippot, and N. Thébaud (2003), Contribution of mantle plumes, crustal thickening and greenstone blanketing to the 2.75–2.65 Ga global crisis, *Precambrian Res.*, *127*, 43–60.

Rudnick, R. L., and D. M. Fountain (1995), Nature and composition of the continental crust: A lower crustal perspective, *Rev. Geophys.*, *33*, 267–309.

Sutcliffe, R. H. (1991), Proterozoic geology of the Lake Superior area, in *Geology of Ontario*, edited by P. C. Thurston et al., pp. 627–658, Ont. Geol. Surv., Toronto, Canada.

Szewczyk, Z. J. (1974), A gravity study of an Archean granitic area north of Ignace, Ontario, M.Sc. thesis, 135 pp., Univ. of Toronto, Toronto, Ont., Canada.

Trehu, A., et al. (1991), Imaging the Midcontinent rift beneath Lake Superior using large aperture seismic data, *Geophys. Res. Lett.*, *18*, 625–628.

Thurston, P. C., I. A. Osmani, and D. Stone (1991), Northwestern Superior Province: Review and terrane analysis, in *Geology of Ontario*, edited by P. C. Thurston et al., pp. 81–142, Ont. Geol. Surv., Toronto, Canada.

Vanderhaeghe, O., and C. Teyssier (2001), Partial melting and flow of orogens, *Tectonophysics*, *342*, 451–472.

West, G. F., and J.-C. Mareschal (1979), A model for Archean tectonism, part I: The thermal conditions, *Can. J. Earth Sci.*, *16*, 1942–1950.

White, D. J., G. Musacchio, H. H. Helmstaedt, R. M. Harrap, P. C. Thurston, A. van der Velden, and K. Hall (2003), Images of a lower-crustal oceanic slab: Direct evidence for tectonic accretion in the Archean Western Superior Province, *Geology*, *31*, 997–1000.

Wilde, S. A., M. F. Middleton, and B. J. Evans (1996), Terrane accretion in the southwestern Yilgarn Craton: Evidence from a deep seismic crustal profile, *Precambrian Res.*, *78*, 179–196.

Williams, H. R. (1990), Subprovince accretion tectonics in the south-central Superior Province, *Can. J. Earth Sci.*, *27*, 570–581.

Williams, H. R., G. M. Stott, P. C. Thurston, R. H. Sutcliffe, G. Bennett, R. M. Easton, and D. K. Armstrong (1992), Tectonic evolution of Ontario: Summary and synthesis, in *Geology of Ontario*, edited by P. C. Thurston et al., pp. 1255–1332, Ont. Geol. Surv., Toronto, Canada.

Yegorova, T. P., V. I. Starostenko, V. G. Kozlenko, and N. I. Pavlenkova (1997), Three-dimensional gravity modeling of the European Mediterranean lithosphere, *Geophys. J. Int.*, *129*, 355–367.

Zegers, T. E., and P. E. van Keken (2001), Middle Archean continent formation by crustal delamination, *Geology*, *29*, 1083–1086.

R. C. Bailey, Department of Physics, University of Toronto, Toronto, ON, Canada M5S 1A7.

B. Nitescu and A. R. Cruden, Department of Geology, University of Toronto, Toronto, ON, Canada M5S 3B1. (bnitescu@geology.utoronto.ca)